

## Modelling of Sediment Transport in Beris Fishery Port

Ardani, S.<sup>1\*</sup> and Soltanpour, M.<sup>2</sup>

<sup>1</sup> Ph.D. Candidate, Texas A & M University, College Station, TX., (Formerly, Graduate Student, K.N. Toosi University of Technology, Tehran, Iran)

<sup>2</sup> Associate Professor, K.N. Toosi University of Technology, Tehran, Iran

Received: 04 Sep. 2013

Revised: 14 Feb. 2015

Accepted: 16 Feb. 2015

**ABSTRACT:** In this paper, the large amount of sedimentation and the resultant shoreline advancements at the breakwaters of Beris Fishery Port are studied. A series of numerical modeling of waves, sediment transport, and shoreline changes were conducted to predict the complicated equilibrium shoreline. The outputs show that the nearshore directions of wave components are not perpendicular to the coast which reveals the existence of longshore currents and consequently sediment transport along the bay. Considering the dynamic equilibrium condition of the bay, the effect of the existing sediment resources in the studied area is also investigated. The study also shows that in spite of the change of the diffraction point of Beris Bay after the construction of the fishery port, the bay is approaching its dynamic equilibrium condition, and the shoreline advancement behind secondary breakwater will stop before blocking the entrance of the port. The probable solutions to overcome the sedimentation problem at the main breakwater are also discussed.

**Keywords:** Bypassing, Crenulate-Shaped Bay, Dynamic Equilibrium, Genesis, HYDROSED, Longshore Sediment Transport (LST), MIKE21

## INTRODUCTION

A coastline is rarely straight; some segments may curve gently in plain and others are indented (Silvester and Hsu, 1997). Crenulate-shaped bays are common features for sandy beaches formed between rocky headlands. Deposition of sediments at the lee side of the headlands may form this type of bays. Beris Fishery Port, located in southeast of Iran, 85 km east of Chahbahar, is one example of the ports constructed in a crenulate-shaped bay. The construction of Beris Fishery Port was finished in 1994. The port has a basin of 25 ha area. The main breakwater is extended from south to north where the secondary breakwater is in east-west direction (Figure 1). The port is suffering

from two mechanisms of sedimentation, that is, sedimentation at the head of the main breakwater and remarkable change of shoreline position at the back of the secondary breakwater (Hajivalie and Soltanpour, 2006). The latter is potentially dangerous because it may block the port entrance if the advancement continues in future (Figure 1).

The objective of this research is to study the sedimentation problem of Beris Port, and the necessity of any remedy. At first, the equilibrium shape of Beris Bay as a crenulate-shaped bay is discussed, and the resources of sediment supply are examined. The parabolic shape equation of Hsu and Evans (1989) is used as the best fitting curve to be fitted to the actual shape of the bay. The existing aerial photographs are compared to understand the long-term evolution of the bay. MEPBAY software

\* Corresponding author E-mail: samira.ardani@gmail.com

(Klein et al., 2003b; Raabe et al., 2010; Hsu et al., 2008) is employed to fit the parabolic curve in a static equilibrium state. Parabolic Mild Slope (PMS) module of MIKE21 by DHI Water and Environment is used in the second part of this paper for the numerical modeling of wave transformation from deep water to shallow areas. Nearshore wave characteristics and the wave direction at the tip of the main breakwater are obtained from the wave transformation model.

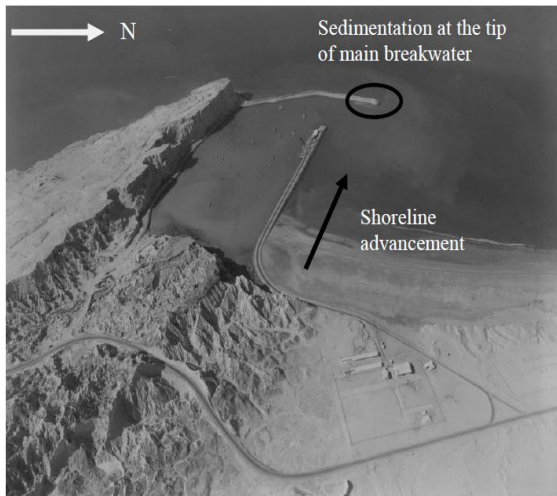


**Fig. 1.** Beris fishing port in 1994.

The third part of this analysis presents the sedimentation condition of the studied domain and modeling of wave-driven currents and sediment transport simulations. HYDROSED, a hydrodynamic and sediment transport numerical model in 2D is employed for the modeling of currents and sediment transport. The calculated potential longshore sediment transport (LST) by HYDROSED is compared with the actual LST rate found from the comparison of hydrographic surveys. Using the actual LST rate as an input value, the GENESIS model of US Army Corps of Engineers (Hanson and Kraus, 1989) is finally applied in the fourth part to predict the time-dependent shape of the shoreline. The LST rate was calibrated to be equal to the actual rate. The results show that the present shoreline position is very close to the dynamic equilibrium state of the bay. At

the end, the recommended solutions for the improvement of sedimentation in this area are presented.

## BERIS EQUILIBRIUM SHAPE

A crenulate-shaped bay consists of three parts, that is, a straight section connected to downcoast headland; middle curve section that can have spiral, parabolic, or hyperbolic tangent shape; and the circular part beside the upcoast headland (Silvester and Hsu, 1997; Klein et al., 2003; Schiaffino et al., 2012). A number of empirical equations have been proposed for the middle part of the curve shape bays. They include logarithmic spiral (Yasso, 1965; Silvester, 1970–1974), parabolic (Hsu and Evans, 1989), modified parabolic shape (Tan and Chew, 1994; Gonzalez and Medina, 1999; Gonzalez et al., 2010), and hyperbolic tangent (Moreno and Kraus, 1999). The parabolic bay-shape empirical formulation of Hsu and Evans (1989) is the most common empirical equation for the planform of crenulate-shaped bays (Gonzalez and Medina, 2001; Silvester and Hsu, 1997; Daly et al., 2014; Klein et al., 2010).

Bays may exist in static or dynamic equilibrium states. In static equilibrium, the downcoast tangent line is parallel to wave crest, there is no longshore component of wave breaking energy and hence no littoral drift within the embayment (Silvester and Hsu, 1997). However, longshore sediment transport exists along the shoreline in dynamic equilibrium, but the shoreline does not change because of the balance between the sediment supply to the bay and sediment removal by waves at the downcoast end. A third case may also be defined, termed as dynamically unstable, where a beach is actively eroding or accreting toward equilibrium state.

The form and stability of crenulate-shaped bays depends on two factors: the

wave condition and the supply of sand to the bay from the upstream bay and from a possible river (Mangor, 2001). Sediment transport mechanism is such that the amount of sand  $Q_B$  from upcoast headland passes and moves along the bay. If a river exists as shown in Figure 2, the sand quantity  $Q_R$  is added to the studied area, and it contributes to the total sediment transport to downcoast. A 2D complicated process governs the sediment transport rate of  $Q_B + Q_R$  to the straight downcoast section of the bay (Figure 2). The direction of sediment transport depends on the incoming wave condition. The bay has stable condition apart from seasonal variations as long as there is no change in  $Q_B + Q_R$ . If the sediment value changes due to the change of upcoast bypass or river sediment input, the bay shape changes resulting accretion or erosion along the coastline.

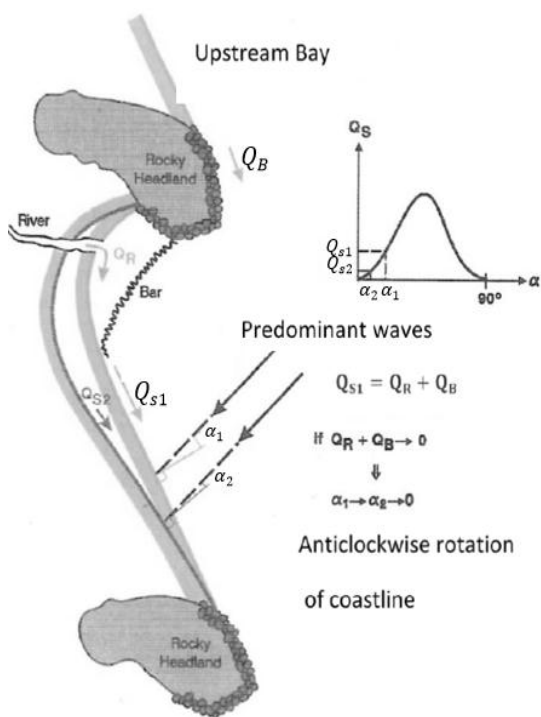


**Fig. 2.** Correlation between shape of a Crenulate bay and transport supply to the bay (Mangor, 2001).

Fitted empirical equations are based on static equilibrium shape with little

sediment transport along the bay. They cannot be accurately applied to define the shorelines in dynamically stable/unstable condition. The prediction of the shoreline in these dynamic conditions is much more complicated, mainly because of the difficulties to access the actual rate of littoral drift.

The comparison of crenulate-shaped bays planform with empirical formulas is an initial step for determining their equilibrium state (Bowman et al., 2009). Hence, fitting formulas are applied to Beris Bay in order to examine the long-term static equilibrium condition of the bay. Iranian Seas Wave Modeling (ISWM) offshore waves are used for the deep offshore wave condition (PMO, 2008). ISWM provides a 12-year hindcast wave data along Iranian coastlines at 6 h intervals. In all, 16070 wave records of ISWM were transformed to shallow waters using Snell formula. Figure 3 shows the 12-year averaged ISWM offshore wave rose at location 61.125 E, 25 N with the depth of about 40 m, and the corresponding transformed nearshore wave rose at the diffraction point at the tip of the main breakwater. The wave rose shows a clear concentration of waves coming from S and SE directions during monsoon season. The small contribution of westerly winter waves has negligible effect on the net longshore sediment transport rate. Moreover, there is a limited seasonal change of shoreline because of the cross-shore sediment transport.

The parabolic shape shows a better fitting to the actual shape of Beris Bay compared to the other fitting curves. The parabolic formula of Hsu and Evans (1989) for bayed beaches in static equilibrium is defined as:

$$\frac{R}{R_0} = C_o + C_1 \left[ \frac{\beta}{\theta} \right] + C_2 \left[ \frac{\beta}{\theta} \right]^2 \quad (1)$$

in which  $R$  : is the line that connects diffraction point to the beach,  $R_0$ : is the control line drawn to the downcoast limit of the beach,  $\theta$ : is the angle between the

crest line and radius, and  $\beta$ : is the angle between control line and the wave crest alignment. The coefficients  $C_0$ ,  $C_1$ , and  $C_2$  depend on  $\beta$  angle.

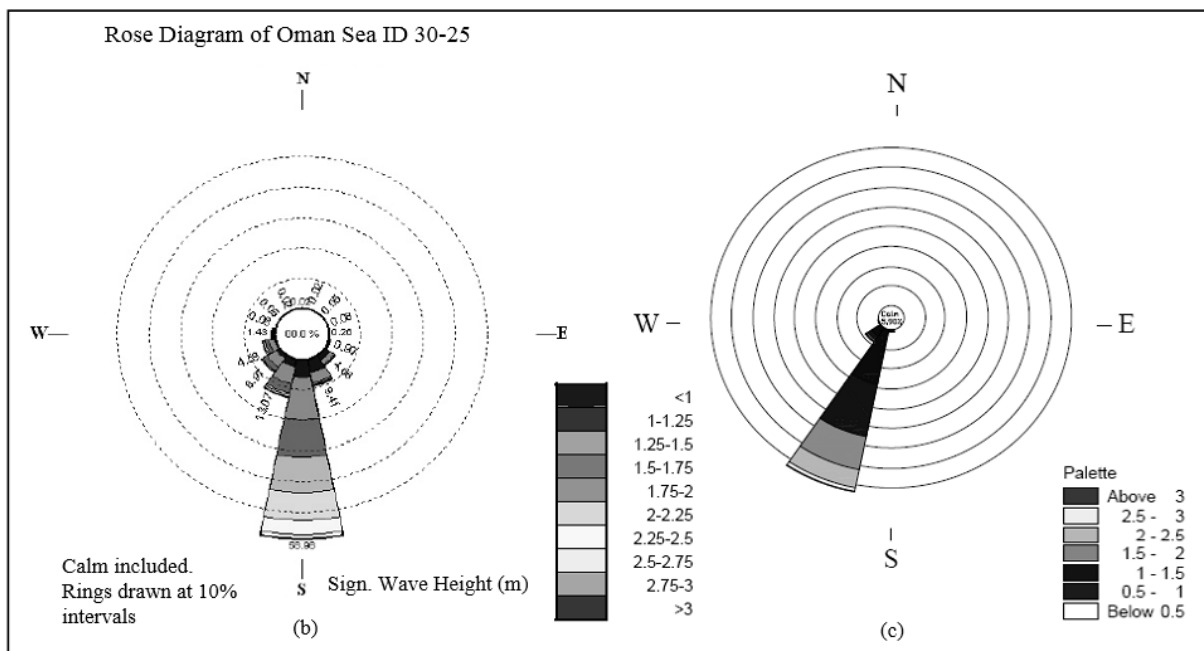
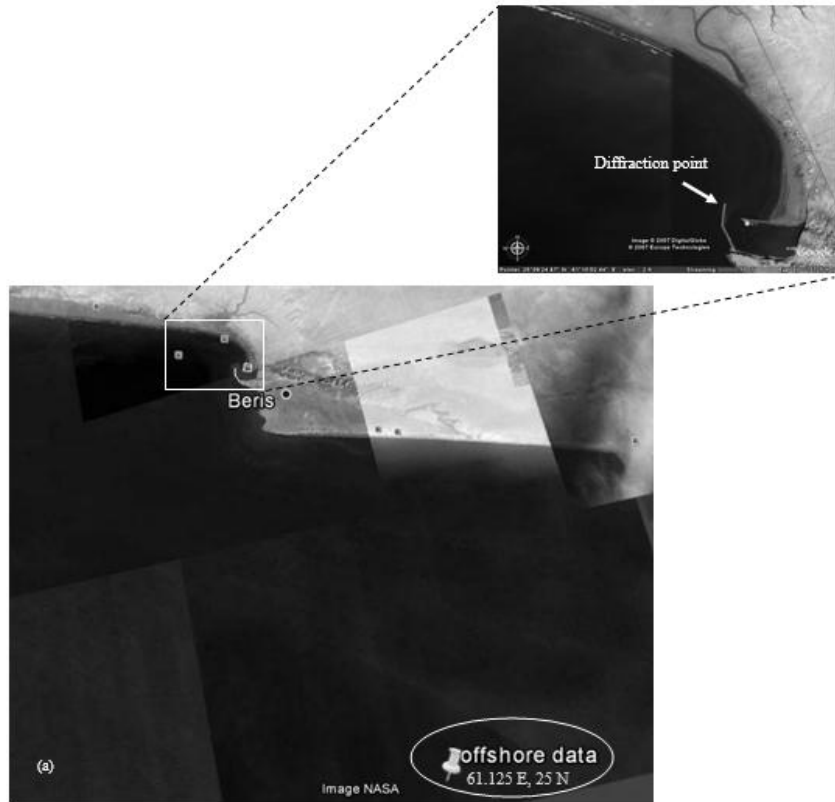


**Fig. 3.** a) Domain of interest, b) ISWM offshore wave rose, c) Nearshore wave rose at the tip of main breakwater.

MEPBAY software, developed by Klein et al. (2003b) is applied here to develop the idealized shoreline in static equilibrium condition. It is based on the parabolic model of Hsu and Evans (1989). The location of upcoast control point is considered at the tip of the breakwater. The downcoast control point is considered at the point where the wave crest is approximately parallel to the downcoast tangent. Based on the frequencies of transformed nearshore wave rose at the diffraction point, the weighted average wave direction was used for the dominant wave direction. Following Silvester and Hsu (1997), a sensitivity analysis was conducted to define the proper location of downcoast control point with little effect on the static equilibrium shoreline of the bay. The results showed that for a control point at the vicinity of the selected location, the corresponding fitted curve to actual bay was not changing within the accuracy of these fitting methods. The uncertainty of the fitted parabolic shape would increase gradually by moving from the downcoast control point toward upcoast (Lausman et al., 2010).

Figure 4 shows the comparison between the actual shape of the bay and the

predicted static equilibrium fitting before and after the construction of the breakwaters. It is observed that the parabolic static curves do not match the actual shape of the bay in both cases although the differences are not large. Because the predicted curve lies landward in comparison to the actual shape of bay, it can be concluded that the shoreline is still moving forward and therefore the bay is not in static equilibrium condition.

The results also reveal the input amount of sediments entering the bay. Two sediment resources are available in the bay, that is, the seasonal river and bypassing sediment at the tip of main headland. The continuous entrance of sediments to the bay implies that the static equilibrium cannot exist. However, the amount of sediments coming out of the seasonal river is not remarkable. If the shoreline is stable at the current state, then it has already reached the dynamic equilibrium. Otherwise, it will continue to change towards the final dynamic equilibrium state. A detailed study of wave, sediment transport, and bathymetry evolution is necessary to investigate the time dependent change of shoreline and to define the final equilibrium state.



**Fig. 4.** Comparison between fitted parabolic model (dash-dot) and actual shape of Beris Bay, a) Before construction of the port – diffraction point at the tip of the headland, b) After construction of the port – diffraction point at the tip of the main breakwater.

## NEARSHORE WAVE MODELING

On irregular bathymetries, proper numerical models are necessary to simulate the complicated wave transformation from deep water to shallow nearshore areas (Silva et al., 2010). The popular SW module of MIKE21 cannot be adopted for wave transformation because diffraction plays a very important role in the simulation of wave transformation in the bay. PMS module of MIKE21 is employed in this study for the wave transformation. PMS is a diffraction-refraction model based on a parabolic approximation to elliptic mild slope equation. According to parabolic approximation, the waves are assumed to propagate in x-direction. MIKE21 employs the method of Kirby (1986) who extended parabolic approximation to the larger angles with respect to x-direction. Different effects of refraction, shoaling, diffraction in perpendicular direction of predominant wave, and energy dissipation due to bed friction and wave breaking are considered in this model.

Berkhoff (1972) defined the elliptic mild slop equation as:

$$\nabla \cdot (CC_g \nabla \phi) + (k^2 CC_g + i\omega W)\phi = 0 \quad (2)$$

where  $\nabla$ : is the 2D gradient,  $c(x, y)$ : is the phase speed,  $c_g(x, y)$ : is the group velocity,  $\phi(x, y)$ : is the velocity potential, and  $\omega$ : is the angular frequency. The median diameter  $d_{50} = 0.2$  mm is used for the calculation of wave friction factor, and Nikuradse roughness parameter is calculated based on Nielsen (1979). Moreover, the symmetrical lateral boundary conditions are specified.

Figure 5 shows the bathymetry of the calculated domain extended up to 20 m water depth. Applying ISWM at offshore boundary, Figure 6 represents calculated nearshore wave rose at three locations along the coast. It is observed that the summation of the wave components is not perpendicular to the shoreline. The resultant oblique wave at the shoreline results to a net longshore sediment transport. This implies that Beris Bay cannot be in a static equilibrium condition.

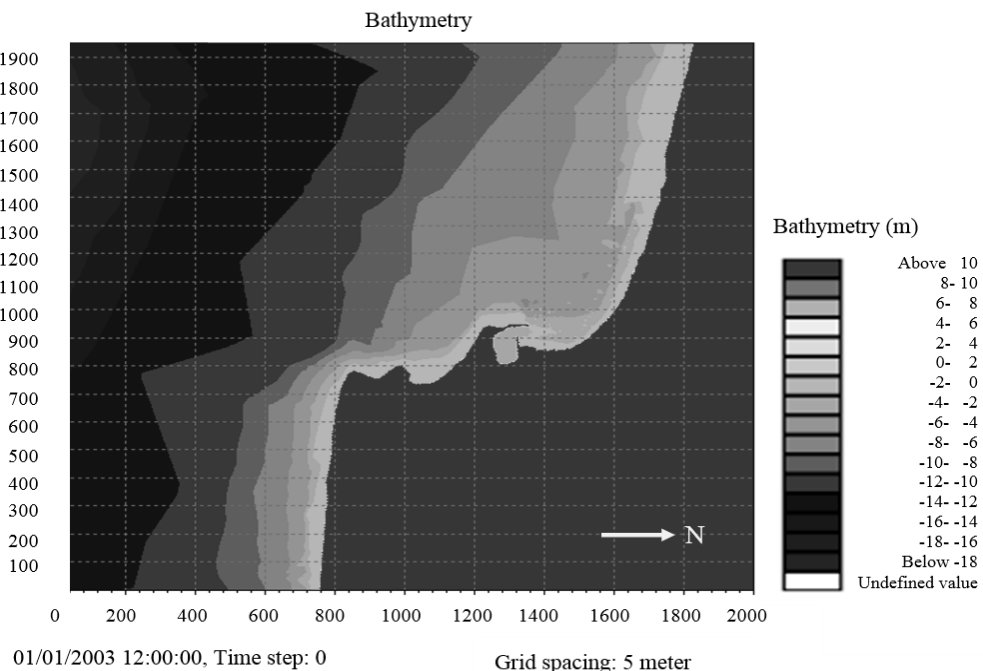


**Fig. 5.** Beris bay bathymetry up to 20 m of water depth in 2005.

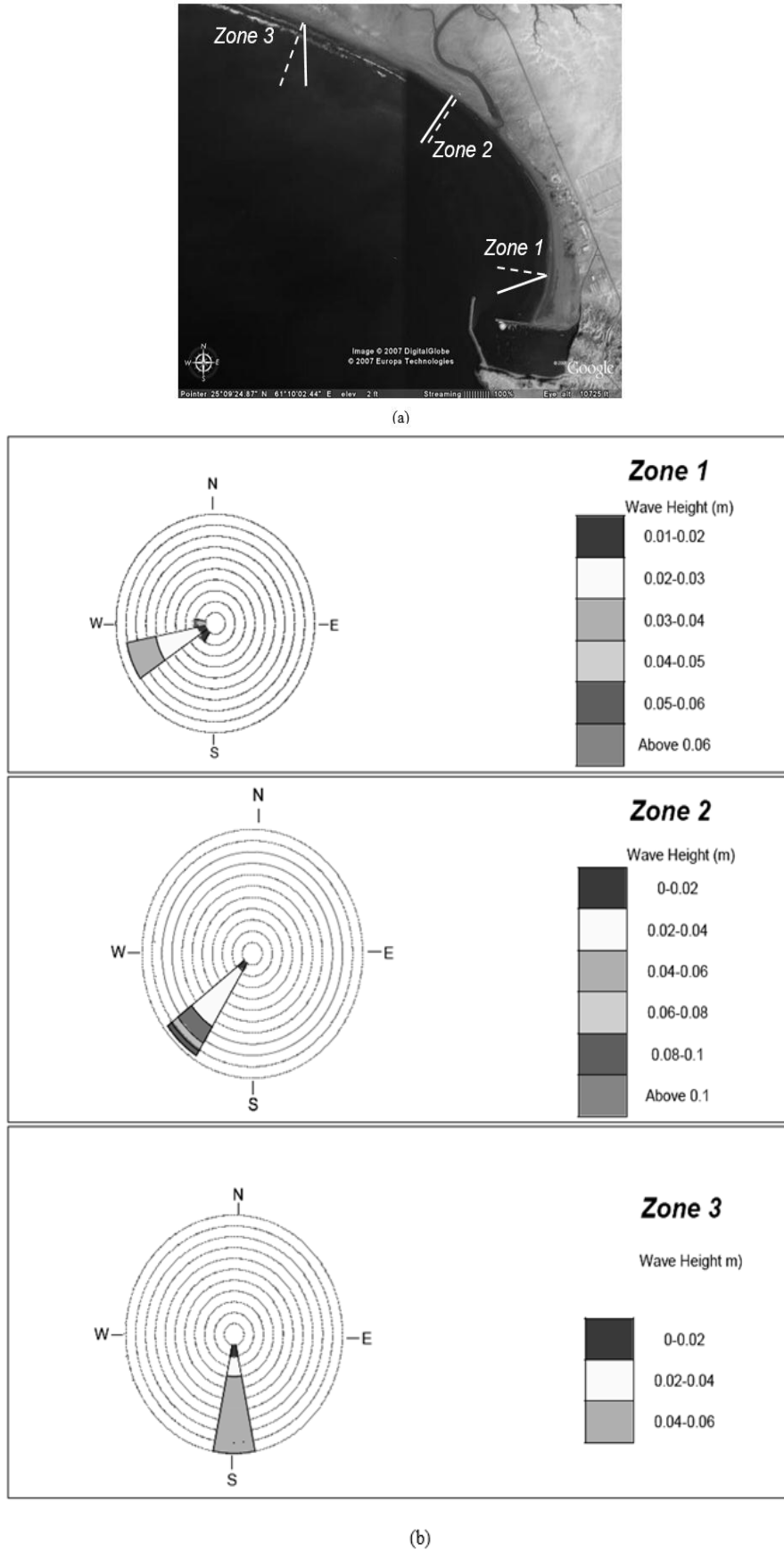


**Fig. 6.** a) The classification of the domain into three zones (Solid line: direction of the waves, Dashed-line: perpendicular to the coastline), b) Nearshore wave roses at different zones of Beris bay.

## SEDIMENTATION

Sedimentation at the north part of the port behind the secondary breakwater started just after the breakwater construction in 1989. Figure 7a presents the shoreline comparison between 1989 and 2001 hydrographical surveys. The comparison shows an accretion volume of about  $1,406,000 m^3$  which is equivalent to about 400 m shoreline change in seaward direction at the secondary breakwater (JWERC, 2002).

AutoCAD Land Desktop 2009, that is, a component of AutoCAD with necessary toolboxes for surveying and civil

engineering, is used for the calculation of accretion and erosion volumes from 2003 to 2005. By comparing these two hydrographic surveys and adding the sediment dredging volume of  $250,000 m^3$  in this time interval, a longshore sediment transport of about  $120,000 m^3 / year$  can be estimated which corresponds to the calculated accretion volume between 1989 and 2001 mentioned before. Figure 7b shows the dredging zone behind the secondary breakwater during the mentioned years.

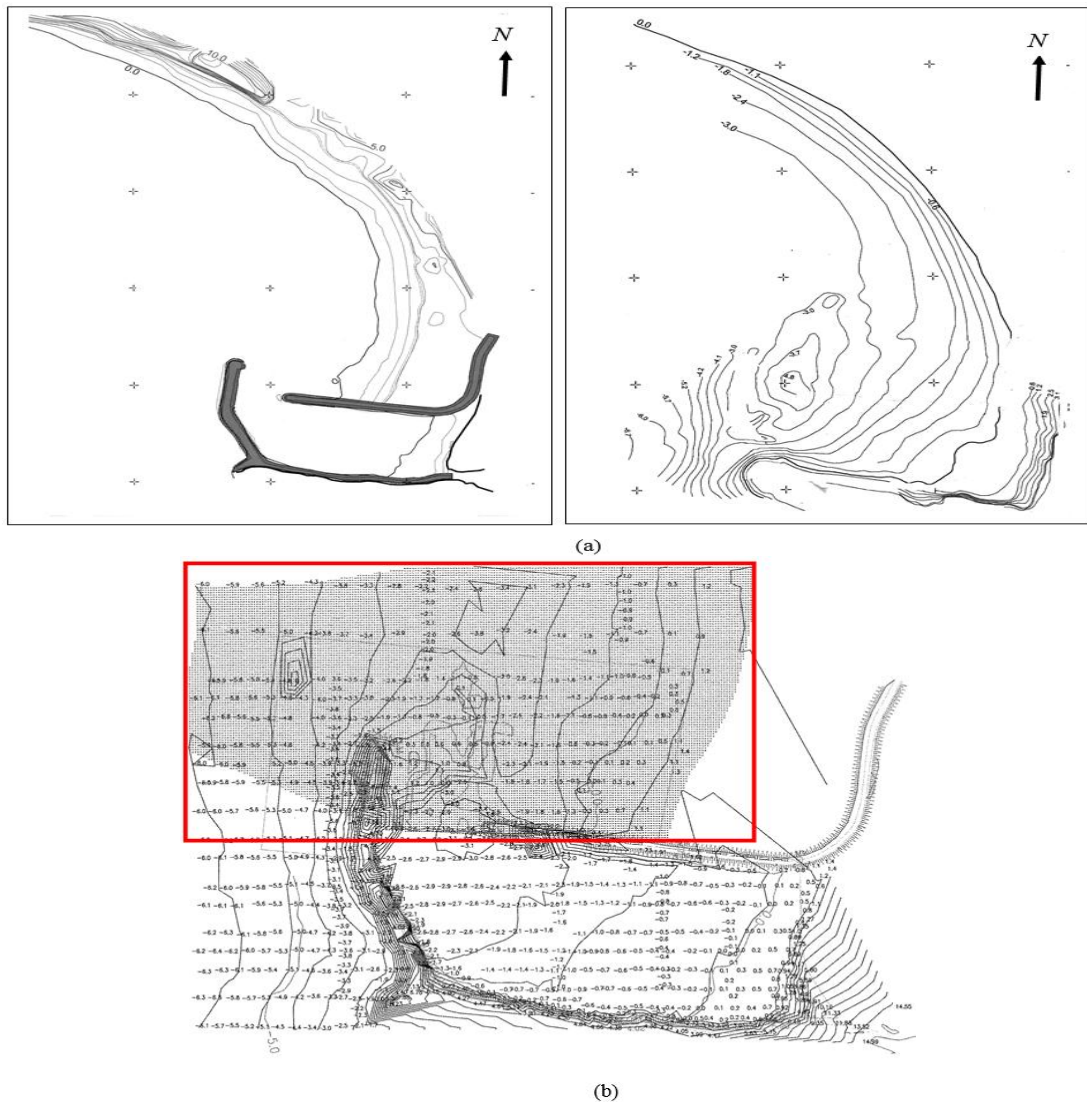


**Fig. 7.** a) Shoreline position at the back of secondary breakwater (up-right: 1989, up-left: 2001) b) Dredged area shown in the rectangular (down-middle).

Two sources of sediment can be distinguished in this area. The first source is the sediment that bypasses at the tip of the major breakwater, and the second one is the sediment coming out from the downcoast seasonal river. Figure 8 shows of the aerial photographs in 1965 and 2003, and Figure 9 represents their

comparison. It is observed that the mouth of the river has slightly moved towards the west, which is in agreement with LST direction downcoast of the port. It can also be concluded that the river sediment has a negligible effect to the input of the sediment to the lee side of the secondary breakwater.

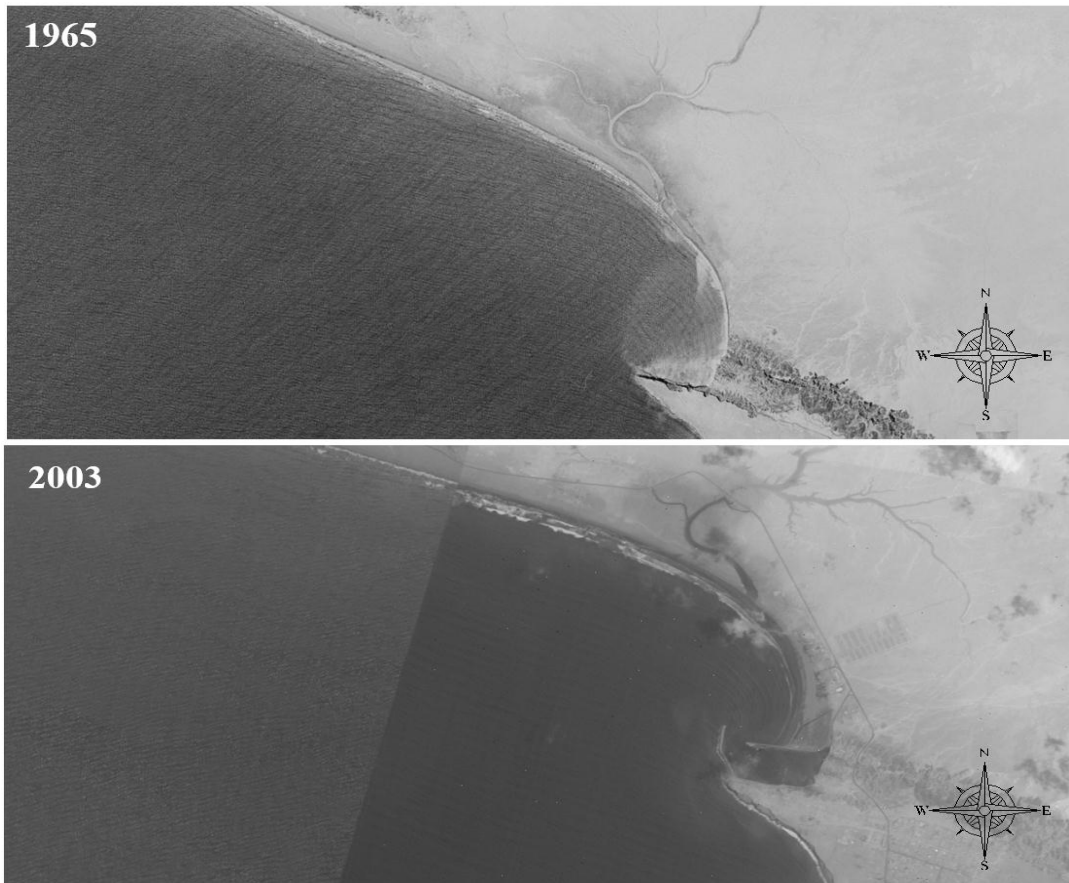


**Fig. 8.** Historic shoreline in beris (up: 1965, down: 2003).

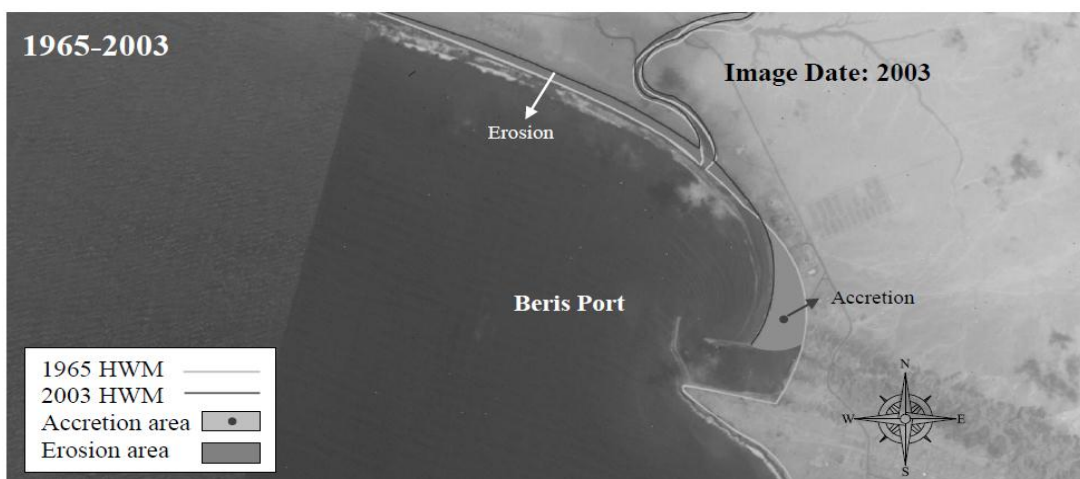


**Fig. 9.** Aerial photograph comparison.

Some part of the sediment passing at the tip of main breakwater settles at the lee side of the main breakwater because of diffraction. Aerial photographs and hydrographical surveys confirm decreasing the water depth at the tip of major breakwater. The rest of bypassing sediment comes to Beris Bay which has resulted to the sedimentation behind the secondary breakwater. However, it is clear that part of the sediment moves toward west direction out of the bay. In a final dynamic equilibrium, there is no more accretion behind the secondary breakwater, and the bypassed sediment will completely moves along the shoreline to the west.

Anticipating the long-term response of the bays with dynamic equilibrium cannot be demonstrated using parabolic bay shape equation (Hsu et al., 2010; Weesakul et al., 2010). In this regard, numerical simulations are employed to capture their sedimentation patterns and long-term shoreline positions.

## HYDROSED MODEL

A 2DH hydrodynamic and sediment transport model, namely, HYDROSED, was used for the analysis of the nearshore currents and sediment transport at the site. HYDROSED is a Baird in-house 2DH hydrodynamic and sediment transport state of the art model for coastal areas. It consists of a spectral wave transformation model (where the wave field is calculated by the spectral energy conservation equation of Karlsson, 1969, with the breaking dissipation term of Isobe, 1987), a hydrodynamic model (Nishimura, 1988) to describe wave generated nearshore currents and circulations (driven by radiation stresses predicted with the spectral wave transformation model) and a sediment transport model presented by Dibajnia et al. (2001). The sediment transport model considers the influence of non-linear orbital velocities and undertow and is based on the sheet flow transport formula of Dibajnia and Watanabe (1992),

which was extended by Dibajnia (1995) to consider suspended transport over ripples as well as the bed load transport. Dibajnia et al. (2001) also conducted a sensitivity test of their model and showed that the model response under various actual nearshore wave environments is satisfactory. For a given wave condition, HYDROSED can provide a full spatial description of nearshore currents and sand transport over the calculation domain.

At first, the bathymetry file, 950\*920 mesh (9.2 km in cross-shore by 9.5 km in longshore) with  $10 \times 10$  m grids was established where the offshore water depth was 20 m. As HYDROSED cannot be applied for a time series of wave conditions to get the actual potential sediment transport rate because of its very high computational time, the model should be applied for the representative cases. Based on the offshore wave rose of Figure 3, HYDROSED was run here for a large monsoon wave of 2 m height and 10 s period arriving from the south direction. The median grain size of 0.2 mm was selected. Figures 10 and 11 show the results of wave and current modeling, respectively. The background shading in Figure 10 shows the distribution of wave heights. The wave refraction in different areas can also be visualized by the direction of vectors. Figure 11 shows the corresponding wave-driven nearshore currents. Background shading in this figure shows the bathymetry and vectors indicate the velocity magnitude and direction of the currents. The established alongshore current bypassing the port entrance towards the south can be observed.

Figures 12 and 13 show the sediment transport rates estimated by HYDROSED. The background shading shows the bathymetry, and the vectors indicate the magnitude and direction of transport. The transport vectors pointing offshore away from the shoreline indicate shoreline erosion under these wave conditions. The

sediment's movements along the bay shoreline reveal that the bay is not in static equilibrium condition.

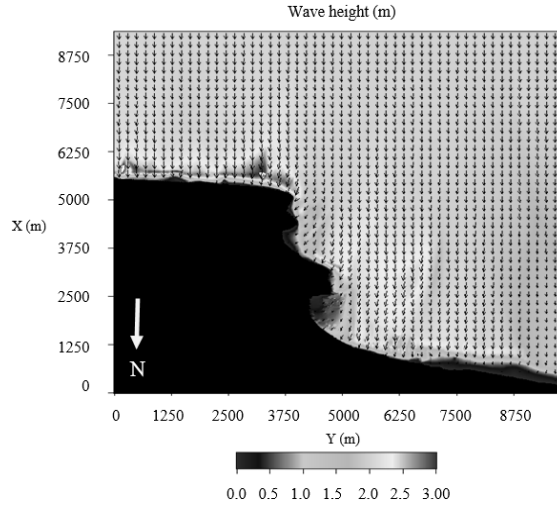


**Fig. 10.** Wave modeling by HYDROSED.

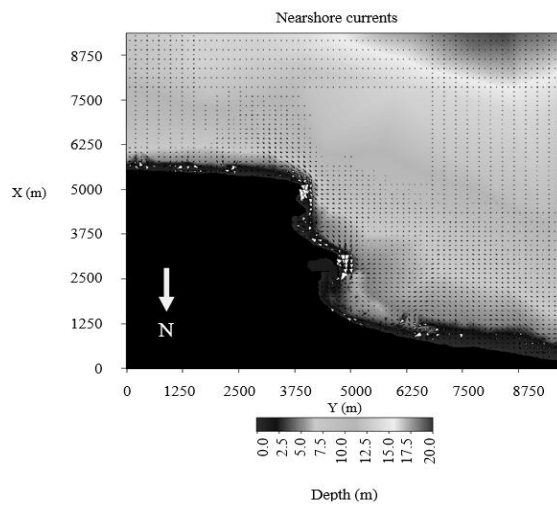


**Fig. 11.** Current modeling by HYDROSED.

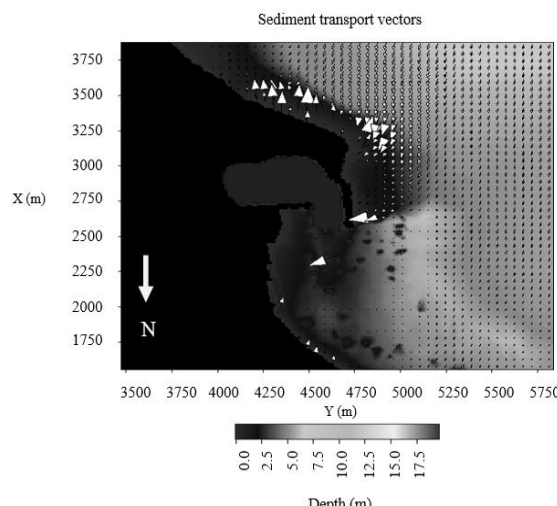


**Fig. 12.** Sediment transport vector by HYDROSED.

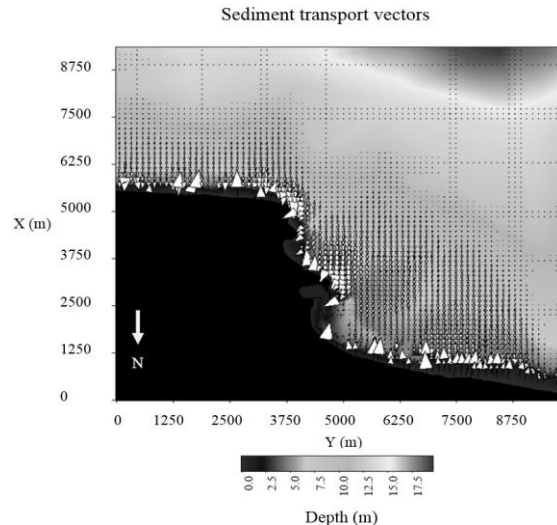


**Fig. 13.** Sediment transport modeling by HYDROSED.

## DYNAMIC EQUILIBRIUM SHAPE OF BERIS BAY

GENESIS numerical software of US Army Corps of Engineers (Hanson and Kraus, 1989) was employed to simulate the long-term evolution of the bay. Input data includes wave condition, two sets of hydrography of studied area, and a file presenting the sediment sources. The model was calibrated by LST rate of 120000 m<sup>3</sup>/year where 2003 and 2005 hydrographical surveys were used to be fitted to the shoreline. The annual longshore sediment transport rate and the yearly predicted shoreline positions were simulated by GENESIS model. Continuing the total time of model runs, the dynamic equilibrium shape of the bay where there is no more change of the shoreline was obtained. Figure 14 shows the dynamic equilibrium shape of Beris Bay in 2011. It is observed that the shoreline advancement stops before the port entrance. This is an important finding which ensures the future navigation through the port entrance. Therefore, the only danger to the port operation is due to the sedimentation at the tip of main breakwater that requires a remedy (Figure 14).

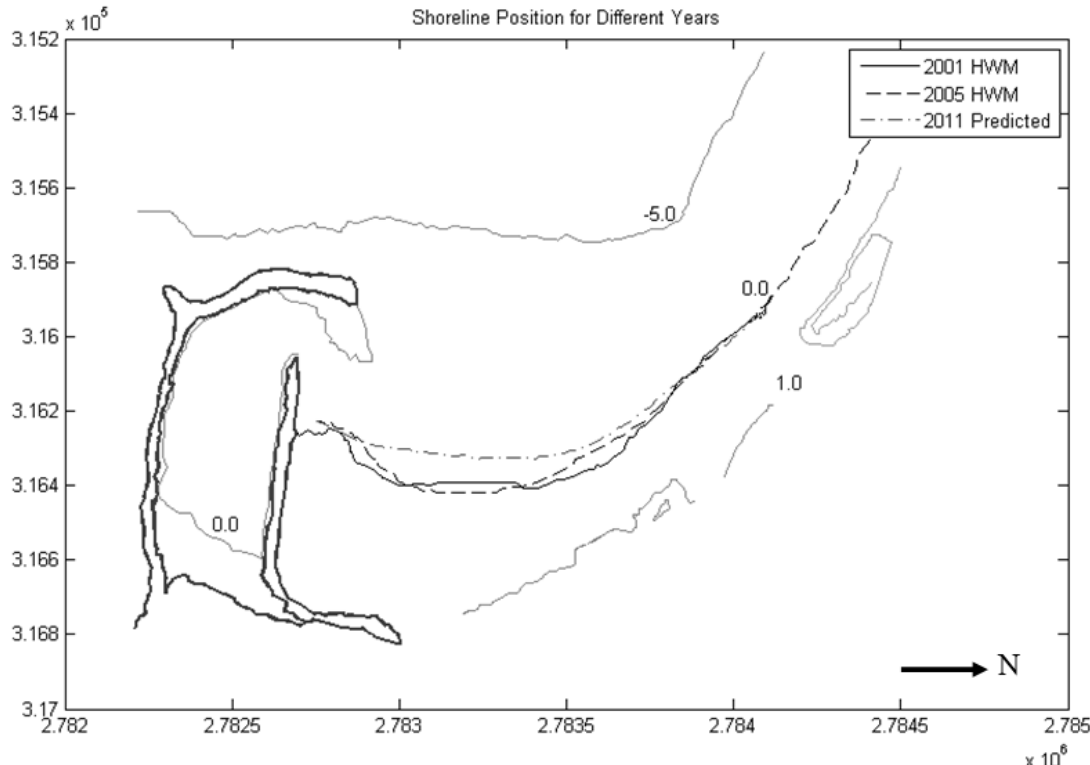


**Fig. 14.** Long term shoreline position (0.0) in dynamic equilibrium (Medium gray line shows shoreline position in dynamic equilibrium- 2011 predicted).

## CONCLUSIONS

LST along the main breakwater and the absence of an updrift fillet is the cause of major sedimentation problem at Beris Fishery Port. The orientation of the main breakwater of the port, which is almost parallel to the shoreline, does not provide a considerable capacity to stop LST, and this has consequently resulted to the bypass of sediment starting in early years after construction. When the sediment reaches the deep water at the tip of main breakwater, a shallow bar at downdrift side of the port is formed transferring the sand to the downstream coast. Moreover, the diffracted waves and tidal currents will push some of the grains towards the harbor through the entrance. As the wave agitation is much less in the protected harbor area, most of this infiltrated sediment ends up on the lee side of main breakwater at the port entrance resulting to the reduction of navigational depth and also the width of the port entrance.

Because the final position of the predicted shoreline does not affect the port entrance, no remedy is necessary for the shoreline advancement behind the secondary breakwater. However, the bypassing LST at the tip of the main breakwater due to diffraction settles at the lee side of the main breakwater (Figures 1 and 14). This affects the navigation at the port entrance. The following options can be considered to overcome this sedimentation:

- A periodic dredging at the head of the main breakwater is sufficient to keep the required depth of navigation. The past experience shows that a dredging period of 15 years is acceptable to maintain the port operation.
- Construction of a groin at the start of the main breakwater (tip of the natural headland) or at the updrift side of the port will stop the LST movement towards the port. This method has already been used to solve the sedimentation problem of the nearby

Pozm Fishery Port, and it can be applied here too. If the head of this groin does not change the diffraction point of the bay, it is expected that erosion will start behind the secondary breakwater, that is, the dynamic equilibrium shape of the bay will change to a static equilibrium. This results to a favorable retreat of the shoreline.

- A westward breakwater segment can be built at the head of the main breakwater to stop bypassing sediment. However, the diffraction point of the bay is changed in this method and it is necessary to derive the final static equilibrium shape of the bay using the new diffraction point, that is, the end of the new added segment.

## ACKNOWLEDGMENT

Thanks are extended to the members of Coastal and Port Engineering Group of JWERC Company for their help in applying PMS module of MIKE21. The authors are also grateful to Dr. Mohammad Dibajnia from Baird & Associates for providing HYDROSED model and his contribution to this paper.

## REFERENCES

- Bowman, D., Guillén, J., Lopez, L. and Pellegrino, V. (2009). "Plan view geometry and morphological characteristics of pocket beaches on the Catalan coast (Spain)", *Geomorphology*, 108(3), 191-199.
- Klein, A.H.F., Vargas, A., Raabe, A.L. A. and Hsu, J.R. (2003). "Visual assessment of bayed beach stability with computer software", *Computers and geosciences*, 29(10), 1249-1257.
- Daly, C.J., Bryan, K. R. and Winter, C. (2014). "Wave energy distribution and morphological development in and around the shadow zone of an embayed beach", *Coastal Engineering*, 93, 40-54.
- Dibajnia, M. (1995). "Sheet flow transport formula extended and applied to horizontal plane problems", *Coastal Engineering in Japan*, 38(2), 179-194.
- Dibajnia, M., Moriya, T. and Watanabe, A. (2001). "A representative wave model for estimation of nearshore local transport rate", *Coastal Engineering Journal*, 43(1), 1-38.
- Dibajnia, M. and Watanabe, A. (1992). "Sheet flow under nonlinear waves and currents", *Coastal Engineering Proceedings*, 1(23), 1-38.
- Gonzalez, M. and Medina, R. (1999). "Equilibrium shoreline response behind a single offshore breakwater", *Coastal Sediments '99*, Vol. 1, 844-859.
- Gonzalez, M. and Medina, R. (2001). "On the application of static equilibrium bay formulations to natural and man-made beaches", *Coastal Engineering*, 43(3), 209-225.
- Gonzalez, M., Medina, R. and Losada, M. (2010). "On the design of beach nourishment projects using static equilibrium concepts: Application to the Spanish coast", *Coastal Engineering*, 57(2), 227-240.
- Hajivalie, F., & Soltanpour, M. (2006). "Beris fishing port, interfering in the equilibrium shape of a bay", *Coastal Engineering*, 30(4), 3843-3850.
- Hanson, H. and Kraus, N.C. (1989). *GENESIS: Generalized model for simulating shoreline change*, Report 1. Technical Reference. No. CERC-TR-89-19-1, Coastal Engineering Research Center, Vicksburg, MS.
- Hsu, J. R., Benedet, L., Klein, A. H., Raabe, A. L., Tsai, C. and Hsu, T. (2008). "Appreciation of static bay beach concept for coastal management and protection", *Journal of Coastal Research*, 24(1), 198-215.
- Hsu, J. R., Yu, M., Lee, F. and Benedet, L. (2010). "Static bay beach concept for scientists and engineers: a review", *Coastal Engineering*, 57(2), 76-91.
- Hsu, J. and Evans, C. (1989). "Parabolic bay shapes and applications", *Institution of Civil Engineers Proceedings*, 87(4) 557-570.
- Isobe, M. (1987). "A parabolic equation model for transformation of irregular waves due to refraction, diffraction and breaking", *Coastal Engineering in Japan*, 30(1), 33-47.
- Jahad Water and Energy Research Company (JWERC) (2002). "Study report of sedimentation at Beris fishery port", Project Report Conducted by JWERC for Shilat Company, Tehran, Iran.
- Karlsson, T. (1969). "Refraction of continuous ocean wave spectra", *Proceedings of American Society of Civil Engineers*, 95(4), 437-448.
- Kirby, J.T. (1986). "Rational approximations in the parabolic equation method for water waves", *Coastal Engineering*, 10(4), 355-378.
- Lausman, R., Klein, A.H. and Stive, M.J. (2010). "Uncertainty in the application of the parabolic bay shape equation: Part 1", *Coastal Engineering*, 57(2), 132-141.

- Mangor, K. (2001). *Shoreline management guidelines*, DHI Water and Environment, 232 p.
- Moreno, L.J. and Kraus, N.C. (1999). "Equilibrium shape of headland-bay beaches for engineering design", *Coastal Sediments '99*, Vol. 1, 860-875.
- Nielsen, P. (1979). *Some basic concepts of wave sediment transport*, Institute of Hydrodynamics and Hydraulic Engineering, Technical University of Denmark.
- Nishimura, H. (1988). "Computation of nearshore current", *Nearshore Dynamics and Coastal Processes*, K. Horikawa, (ed.), University of Tokyo Press, Tokyo, Japan, 271-291.
- Port and Marine Organization (PMO). (2008). *Iranian seas wave modeling (ISWM)*, Vol. 2 Persian Gulf and Oman Sea, General Directorate of Coast and Port Engineering, (in Persian).
- Raabe, A.L., Klein, Antonio H da F, González, M. and Medina, R. (2010). "MEPBAY and SMC: software tools to support different operational levels of headland-bay beach in coastal engineering projects", *Coastal Engineering*, 57(2), 213-226.
- Schiaffino, C.F., Brignone, M. and Ferrari, M. (2012). "Application of the parabolic bay shape equation to sand and gravel beaches on Mediterranean coasts", *Coastal Engineering*, 59(1), 57-63.
- Silva, R., Baquerizo, A., Losada, M.Á. and Mendoza, E. (2010). "Hydrodynamics of a headland-bay beach—nearshore current circulation", *Coastal Engineering*, 57(2), 160-175.
- Silvester, R. (1970). "Growth of crenulate- shaped bays to equilibrium", *Journal of the Waterways, Harbors and Coastal Engineering Division*, 96(2), 275-287.
- Silvester, R. (1974). *Coastal engineering*, Elsevier, Amsterdam.
- Silvester, R. and Hsu, J.R. (1997). *Coastal stabilization*, World Scientific, Singapore.
- Tan, S. and Chiew, Y. (1994). "Analysis of bayed beaches in static equilibrium", *Journal of Waterway, Port, Coastal, and Ocean Engineering*, 120(2), 145-153.
- Weesakul, S., Rasmeemasmuang, T., Tasaduak, S. and Thaicharoen, C. (2010). "Numerical modeling of crenulate bay shapes", *Coastal Engineering*, 57(2), 184-193.
- Yasso, W.E. (1965). "Plan geometry of headland-bay beaches", *Journal of Geology*, 73(5), 702-714.